THE JOURNAL OF PHYSICAL CHEMISTRY C

Article

Cite This: J. Phys. Chem. C 2019, 123, 28201−28209

pubs.acs.org/JPCC

Molecular Insights into the Role of Electronic Substituents on the Chemical Environment of the $-CH_3$ and >C═O Groups of Neat Liquid Monomers Using Sum Frequency Generation Spectroscopy

Uvinduni I. Premadasa,[†] Narendra M. Adhikari,[†] and Katherine Leslee A. Cimatu*

Department of Chemistry and Biochemistry, Ohio University, 100 University Terrace, 136 Clippinger Laboratories, Athens, Ohio 45701-2979, United States

Supporting Information

ABSTRACT: In this work, the substitution of ethyl methacrylate monomers is used as an approach to investigate the effects of electron withdrawing group substituents to their conformation at the two interfaces using sum frequency generation (SFG) spectroscopy. Cyano (−CN), hydroxyl (−OH), chloro (−Cl), and bromo (−Br) groups are substituted at the ethyl end of the methacrylate backbone to replace one H atom. Then, these neat substituted monomers are monitored at both the air−liquid (AL) and solid−liquid (SL) interfaces. The SFG spectra were recorded at different polarization combinations and infrared regions to probe specific different vibrational modes. The spectral results show relative changes in the orientation of the α-methyl (α-CH_3) group with respect to variations in the substituents. This conformational change can be subsequently correlated to the carbonyl (>C═O) group, which is structurally positioned close to the α-CH_3 group. The resulting intermolecular interactions in a condensed phase, especially between the α-CH_3 group and the substituent in close proximity, caused spectral changes obtained at the AL interface. These spectral changes revealed variations in (1) the intensity of methyl Fermi resonance mode at ∼2935 cm^{-1} relative to the α-CH_3 symmetric stretch, (2) the tilt angle of the α-CH_3 group relative to the carbonyl group, and (3) the intensity of the C═O stretch at ∼1720 cm^{-1}. The changes in the oscillator strengths of these vibrational modes suggested that these intermolecular interactions were triggered by the presence of these substituents in space. In addition, the overall conformation was driven by the strength and direction of the dipole moment. When Si−OH oscillator is introduced through hydrogen bonding interaction at the hydrophilic SL interface, a change in the C═O stretch SFG signal clarifies the significant contribution of the dipole moment in the changes observed at the AL interface. The key insight shows the importance of SFG spectroscopy as a tool to probe the small structural modifications of neat compounds.

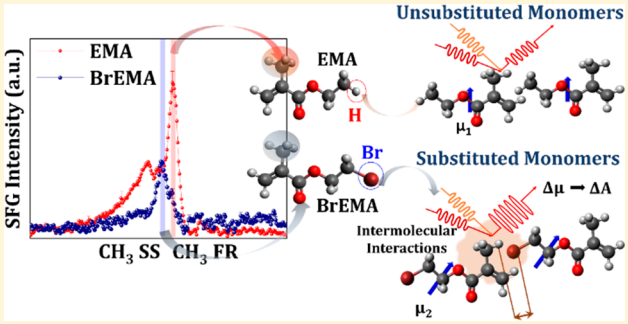

INTRODUCTION

Research studies in predicting and interpreting substituent effects on physicochemical properties and reactivities of organic molecules have continued with unabated diligence. In general, if an electron withdrawing or donating group is present in a molecule, a change in the local dipole is expected to affect the properties which are driven by the structural components of the compound. Many theoretical and experimental studies have been carried out to focus on the function of an electronic substituent at a reaction center and its influence on the reactivity of the compound.[1−3] For example, the substitution of CN for H increases the ethyl ester hydrolysis by a factor of 20.[1] Additionally, a study carried out by Valenti and co-workers showed that substituents affect the thermal behavior of thermotropic polymers.[4] It is noteworthy to know that small molecular changes in structure have a significant contribution to the resulting macroscopic properties of such materials.

However, the investigation of the effects of the electronic substituents in neat liquids at a molecular level have not yet been fully investigated, especially in terms of the conformations of the molecules at different interfaces. Such studies can also be beneficial to liquid−liquid interfacial studies.[5] The predictions and evaluations performed for the bulk studies have, in general, provided a boost in physical organic chemistry.[1−3,6] Nonetheless, it is equally, fundamentally important to examine substituent effects at different interfaces because the structural integrity, function, and dynamics of a material can be distinct from those of the same material in the bulk and can be significant to many interfacial phenomena.[7,8] Thus, we chose methacrylate-based monomers, small molecules with a small degree of complexity, as model compounds to study such substituent effects at surfaces and interfaces (Figure 1). The substitution of the ethyl methacrylate monomer serves as an ideal approach to monitor conformational changes when probing for different functional groups

Received: August 15, 2019
Revised: October 21, 2019
Published: October 29, 2019

DOI: 10.1021/acs.jpcc.9b07816
J. Phys. Chem. C 2019, 123, 28201−28209

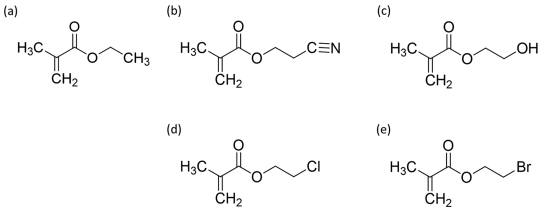

Figure 1. ChemDraw structural representations of the methacrylate-based monomers.

such as C═O, C═C, and α-CH_3. Another advantage of using these monomers is their ability to undergo free radical polymerization because of the vinyl (═CH_2) group.[9,10] In polymerization reactions, experimental factors such as initiators, polymerization temperatures, solvents, and emulsifications are identified and optimized for high yield, better selectivity, and faster reaction kinetics. To describe these parameters which better demonstrate the significance of neat monomers is when polymerization reactions are performed at the liquid−liquid interface. Having said that, this study of polymer monomeric compounds has great relevance to reactions and polymerizations at the liquid−liquid interface between two immiscible liquids, as reported in a review by Landfester and co-workers in 2016.[11] This review summarizes several studies on different emulsification techniques, reactions at interfaces, and even polymerization at the droplet interface. The authors emphasize the significance of an interface which is described as a confined area between two phases from which new products are formed from an interface-assisted reaction. These result from accelerated reactions due to better selectivity, faster kinetics, and more product yield. In this case, the interface provides larger surface area for reactions to occur from which reactions can be conducted in a steady-state environment or mechanically stirred solution. The two immiscible liquids also act as carriers for initiators and reactants which improved selectivity. For example, monomeric compounds delivered from either phase can be positioned in close proximity[12] to the interface. Thus, promoting the reaction which then generates the polymer; a polymer that can be soluble or insoluble in any of the phases. A good example was presented by Manna and Kumar in 2013.[13] They presented an exhaustive analysis in order to understand how existence of an interface affects the "on water" organic reactions' mechanism. The organic reaction focused on using cyclopentadiene and alkyl acrylate and was enhanced by the formation of droplets via stirring in water. By changing the alkyl chain, the hydrogen bonding capability was reduced from methyl, to ethyl, to butyl acrylate. The hydrogen-bonding capability of both the cyclopentadiene and alkyl acrylate with the neighboring water molecules of the droplets induced changes at the heterogeneous conditions of the reaction. They also reported temperature-dependent analysis in order to understand the effect of decreasing H-bonding which resulted in decreasing the exothermic nature of the enthalpy and the entropy. Another study on cationic polymerization emphasized finding ideal reactions at the lowest possible temperatures to avoid transfer reactions which are common for vinyl monomers.[14,15] Ganachaud and co-workers focused on enabling the use of aqueous environment for polymerization reactions with less strict and simpler experimental conditions.[15] To summarize, experimental conditions we used for our neat monomers at the air−liquid interface during our measurements are relevant in understanding how proximity, conformations, and intermolecular interactions affect polymerization reactions in situ or at different interfaces.

We analyzed this series of methacrylate monomers using sum frequency generation (SFG) spectroscopy, a nonlinear vibrational spectroscopic technique.[16,17] SFG spectroscopy is selective and sensitive in probing conformational changes at surfaces and interfaces using different polarization configurations.[18−20] The detailed theory and background of SFG spectroscopy are reported elsewhere.[16,17,21−23]

In our previous work, we reported the orientation of the α-CH_3 group for a couple of selected bulky-substituted methacrylate-based monomers. We obtained the orientation distribution angles of the α-CH_3 symmetric stretch at ∼30° and ∼60° for the methoxy (O−CH_3) and phenoxy (O−Ph) group substitutions, respectively. We also reported π-stacking interactions which played an important role in how the phenyl group affected the overall monomer conformation and the surface tension of the monomer at the air−liquid (AL) interface.[24] In this study, we evaluated the SFG spectra to obtain insight into the resulting conformational changes of our substituted monomers with electron withdrawing groups (EWGs). We believe, with this EWG substitution, a clearer conformational change for the α-CH_3 group can be obtained from the two different interfaces because the ethyl-substituted group does not interfere with the methyl (CH_3) vibrational modes. Figure 1 shows the chemical structure of five monomers: ethyl methacrylate (EMA), 2-cyanoethyl methacrylate (CNEMA), 2-hydroxyethyl methacrylate (HEMA), 2-chloroethyl methacrylate (ClEMA), and 2-bromoethyl methacrylate (BrEMA).

METHODS

The EMA and HEMA monomers were purchased from Sigma-Aldrich (St. Louis, MO) and were purified before use. The CNEMA, ClEMA, and BrEMA monomers were synthesized in-house and characterized to ensure purity and structure. The detailed description of the synthesis of monomers, ^{1}H NMR and ^{13}C NMR characterizations (Figures S1−S3), sample preparation, and SFG experimental methods at the AL and solid−liquid (SL) interfaces are provided in the Supporting Information. Dilute monomer solutions (60 mL, 8.0 mM, 6.0 mM, and 4.0 mM) were prepared in H_2O. The SFG spectra were recorded with SSP and PPP polarization combinations in the CH region and CO region.

Fourier transform infrared (FTIR) spectrometry (Shimadzu IRAffinity-1S, Columbia, MD) was utilized for the IR characterization. Potassium bromide windows were used as plates to hold the liquid monomers. An R-3000 spectrometer (PhotoniTech Pvt Ltd., Singapore) was used for the Raman characterization of the monomers. The Du Noüy ring method was used to measure the surface tension of methacrylate monomers at the AL interface using a surface tensiometer (CENCO-DuNouy interfacial tensiometer no. 70545, Central Scientific Co., Chicago, IL). The detailed experimental methods for surface tension measurements are reported in our previous paper.[24]

RESULTS AND DISCUSSION

Initially, the SFG spectra of the EMA, CNEMA, HEMA, ClEMA, and BrEMA monomers were collected using SSP and PPP polarization combinations in the CH vibrational region

DOI: 10.1021/acs.jpcc.9b07816
J. Phys. Chem. C 2019, 123, 28201−28209

(2900−3100 cm^{-1}) at the AL interface (Figure 2). The SFG experimental method is described in the Supporting

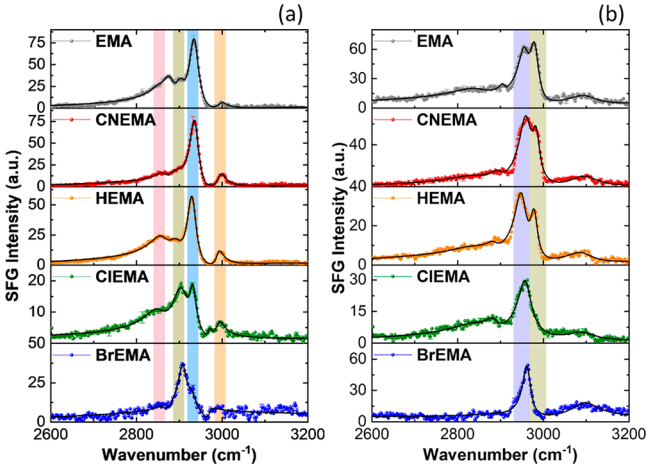

Figure 2. SFG spectra of substituted methacrylate monomers at the air−liquid interface at (a) SSP and (b) PPP polarization combinations.

Information. In the SSP spectra of monomers (Figure 2a), the methylene symmetric stretch (CH_2 SS, ∼2850 cm^{-1}),[25] α-methyl symmetric stretch (α-CH_3 SS, ∼2900 cm^{-1}),[26] CH_3 Fermi resonance (CH_3 FR, ∼2930 cm^{-1}),[27] and alkene methylene symmetric stretch (=CH_2 SS, ∼3000 cm^{-1})[28] vibrational modes are observed. The CH_3 FR mode (blue highlight, Figure 2) is evident in the SSP spectrum of the unsubstituted EMA monomer. After analysis, we found the SSP spectra of the substituted CNEMA and HEMA monomers had similar spectral profiles to the EMA monomer where CH_3 FR dominates each spectrum. On the other hand, the α-CH_3 SS mode (green highlight, Figure 2) is visually more prominent in the SSP spectra of the ClEMA and BrEMA monomers, as supported by the amplitude values obtained from the fittings (available in Table S1, Supporting Information). In the general definition, the Fermi resonance mode is generated due to the CH_3 SS vibration splitting by Fermi resonance with an overtone of a CH_3 bending mode.[29] The clear intensity differences of the CH_3 FR vibrational modes of ClEMA and BrEMA monomers from the EMA monomer suggest these were initially caused by a change in the overall conformation at the AL interface. Nevertheless, Fermi interactions, in general, are sensitive to a small conformational change of a molecule induced by its interaction with the chemical surroundings.[30]

The analysis of the PPP spectra of CNEMA and HEMA monomers shows their spectral profiles to be similar to what was obtained from the EMA monomer. Both the in-plane (IP) and out-of-plane (OP) α-CH_3 asymmetric (AS) stretches (2960 and 2975 cm^{-1}, respectively)[23] have discernible contributions to the spectra (see Figure 2b). IP and OP CH_3 AS stretches are usually unresolved.[17] However, in our case, we can resolve the two peaks from each other. The relative intensity ratio between the IP and OP AS stretches increases from EMA to CNEMA and HEMA. The intensity change means that, since the polarization of both incident beams is parallel to the incident plane, a combination of both the IP and OP AS stretches is probed by the p-polarized visible and IR beams while only p-polarized SFG signal is recorded. This means that both vibrational modes also lie parallel to the incident plane.[31] However, in the PPP spectra of ClEMA and BrEMA, only the in-plane α-CH_3 AS mode is observed. This observation suggests most of the in-plane α-CH_3 AS stretches are positioned along the plane of incidence while a reduced contribution from the OP α-CH_3 AS vibrational mode was observed when compared to CNEMA and HEMA.

Thus, when the FR signal at the SSP spectra is more prominent, the contributions from both IP and OP α-CH_3 AS stretches are more evident. On the other hand, when the FR signal contribution is reduced, the IP α-CH_3 AS stretch is more pronounced when compared to the OP α-CH_3 AS stretch. If that is the case, the replacement of H with substituents has resulted in a conformational change of the interfacial monomers. Closer spectral analysis of the BrEMA monomer shows that the α-CH_3 SS vibrational mode is positioned perpendicular to the vibrational motion of the IP α-CH_3 AS stretch. Therefore, the chemical environment in the presence of the Br substituent created a more ordered arrangement of the interfacial monomers. The asymmetry condition for SF activity also enables estimation of the degree of order or conformation of the interfacial molecules such as these monomers at a molecular level.[17] However, this observation can also be explained when degeneracy is reduced between the IP and OP CH_3 AS stretches because of physical perturbation due to a change in the chemical environment provided by the substituents. Using the same reasoning, the reduction in the FR signal from H to −CN, −OH, −Cl, and −Br can also be clarified by the fact that α-CH_3 SS splitting due to FR interaction with an overtone of the CH_3 SS bending mode is when energy states are equal between these two modes. Additionally, the intensification of the vibrational mode positioned at ∼2935 cm^{-1} can be explained by the contribution of the CH_3 SS fundamental mode to the overtone band itself. For example, as shown in the BrEMA SSP spectrum (Figure 2), the FR signal has decreased in intensity. Therefore, the FR interaction between the fundamental mode and the normally weak overtone of the CH_3 SS bending mode has been reduced which means there is a slight energy mismatch between the two modes; two bands are not symmetrically placed about the expected position for the overtone and less contribution from the fundamental mode. This occurrence is due to the reduced perturbation introduced by changing H with the Br substituent.[32] Figure 3a represents the reduced degeneracy of the energy states for the fundamental mode and the overtone of the CH_3 bending mode with the presence of Br substituent in comparison to the absence of substituent. Overall, the frequency of the fundamental vibration (α-CH_3 SS) is sensitive to changes in its environment; changes in the solvent and its current liquid state can affect the intensity of the FR vibrational band.[28] Thus, the modification of the monomer by varying the substituents resulted in decreasing the intensity of the FR signal positioned at ∼2930 cm^{-1} of the SSP spectrum (Figure 2).

These observations are results of noncovalent intermolecular interactions occurring through space between the α-CH_3 group and the substituents with both in close proximity. As shown in Figure 3b, changing H with Br substituent in the monomer allows the change in the polarity of the α-CH_3[17,33] of another neighboring monomer, thus affecting the overall dipole moment (μ) of the molecule and the strength of the oscillator bands (A).

DOI: 10.1021/acs.jpcc.9b07816
J. Phys. Chem. C 2019, 123, 28201−28209

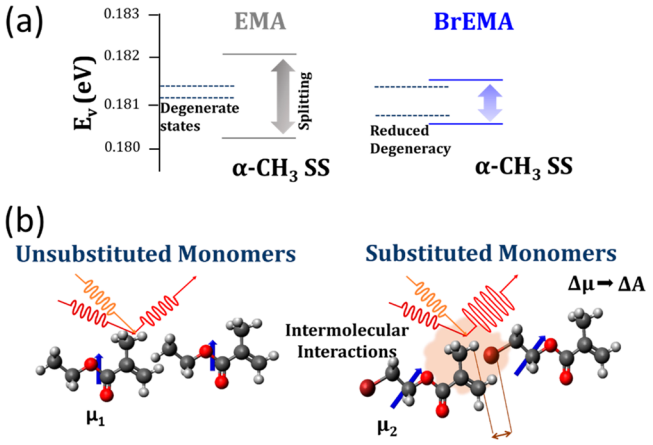

Figure 3. (a) Representation of α-CH_3 SS splitting due to FR interaction with an overtone of the CH_3 bending mode when two states are degenerate (for EMA monomer) and when there is reduced degeneracy in the two states (for BrEMA monomer). (b) Representation of the affected oscillator band strength due to a change in the polarity of the α-CH_3 group due to the presence of the substituents in close proximity.

To prove the effect of proximity, we prepared aqueous solutions of three methacrylate-based monomers (EMA, CNEMA, and BrEMA) to spatially separate the monomer molecules from each other. We hypothetically reduced the number of monomer−monomer interactions as a function of concentration in water. This approach was used in order to investigate whether the reduction of the FR signal could be due to field effects as driven by the close proximity of the α-CH_3 group and the substituent (Figure S4).

The neat EMA monomer has its most intense peak at ∼2935 cm^{-1} assigned for CH_3 FR. In the presence of water molecules, two peaks at ∼2905 (CH_3 SS) and ∼2967 cm^{-1} (CH_3 AS) become apparent. Then, for the CNEMA neat monomer, the FR peak has remained in the same position at ∼2935 cm^{-1} from neat monomer to 8, 6, and 4 mM aqueous solutions of CNEMA monomer. The characterization of the neat Br-substituted monomer at the AL interface has resulted in a peak at ∼2907 cm^{-1}. However, as we introduced water molecules, three distinct peaks appeared in the SSP spectra and its spectral profile has remained similar for all aqueous solutions of the BrEMA monomer. As we have predicted, the peak positioned at ∼2950 cm^{-1} has appeared and is a result of the increased FR interaction between the CH_3 SS and an overtone of the CH_3 bending mode. The additional two peaks are from the CH_2 (∼2850 cm^{-1}) and CH_3 (∼2880 cm^{-1}) vibrational modes. The PPP spectra of all aqueous solutions of the three monomers supported the assignment of the peaks in the SSP spectra. The spectral changes observed in EMA and BrEMA monomers in water compared to their neat forms were a result of the water molecules surrounding the monomers which at the end affected the orientation of the monomers. Thus, these spectral changes are probably due to (1) interference effects as a result of different orientations of the CH vibrational modes and (2) contribution of resonant response of water via second-order resonant susceptibility ($\chi^{(2)}$) and the third-order optical properties of the bulk water ($\chi^{(3)}$).

In SSP spectra of EMA monomer in water (Figure S4a, the disappearance of the α-CH_3 FR peak at 2935 cm^{-1} and the appearance of a peak at 2967 cm^{-1} could be a result of the destructive interference between the α-CH_3 FR and α-CH_3 AS modes. This is further proven by the PPP spectra, where the peak positioned at ∼2967 cm^{-1} is assigned as the α-CH_3 AS. To test the effect of contribution from resonant response of water via $\chi^{(2)}$ or $\chi^{(3)}$ on the observed spectral changes when going from neat EMA monomer to aqueous EMA monomer, a control experiment was carried out using 8 mM EMA in water with 5% (w/v) salt. As the salt concentration was increased, the combined contributions from the second-order resonant susceptibility ($\chi^{(2)}$) and the third-order optical properties of the bulk water given by a $\chi^{(3)}$ term; the SFG signal from $\chi^{(2)}$ and $\chi^{(3)}$ was reduced.[34] From the spectra (Figure S5), it was clear that the spectral profile changes when $\chi^{(2)}$ or $\chi^{(3)}$ contributions are reduced by adding salt. This possibility explains the disappearance of the CH_3 FR peak and, at the same time, the appearance of the CH_3 AS positioned at ∼2965 cm^{-1}. Looking closely at spectra, the spectral profile of EMA monomer in water with 5% salt shows a convoluted shoulder of the CH_3 FR (∼2950 cm^{-1}) and the CH_3 AS (∼2965 cm^{-1}). The observation of the 2950 cm^{-1} peak is a result of incomplete suppression of the $\chi^{(2)}$ and $\chi^{(3)}$ signals at 5% salt concentration.

However, such an FR peak shift was not observed in CNEMA aqueous samples compared to its neat form (Figure S4b). Interestingly, the spectral profile for CNEMA neat and aqueous samples is the same, especially for the peak positioned at ∼2935 cm^{-1}. This indicates that water−monomer and monomer−monomer interactions have the same effect on the orientation of the monomer at the air−liquid interface.

In SSP spectra of BrEMA monomer in water (Figure S4c), the disappearance of the α-CH_3 FR peak at 2935 cm^{-1} and appearance of a peak at 2950 cm^{-1} could also be a result of destructive interference between the α-CH_3 FR and α-CH_3 AS mode. However, in the PPP spectra, the most distinct peak positioned at ∼2965 cm^{-1} is assigned to α-CH_3 AS. Therefore, CH_3 AS in the SSP spectrum should be positioned at ∼2965 cm^{-1} as well.[10,21,24] In addition, the peak at ∼2950 cm^{-1} is the most apparent peak in the SSP spectrum.[10] Therefore, it can be concluded that the peak at 2950 cm^{-1} in the SSP spectrum of BrEMA in water is not coming from the α-CH_3 AS but is a result of the increased FR interaction between the CH_3 SS and an overtone of the CH_3 bending mode. The peak shift from ∼2935 to 2950 cm^{-1} is an indication of the FR sensitivity to changes to its surroundings. However, it is also true that the difference in the orientation of the α-CH_3 group, as a neat liquid, and in water, leads to an apparent peak shift.[35] This explanation still supports the spectral change and it can still be explained that the change in the orientation of the monomer was due to the presence of water molecules which then separates the monomer molecules from each other.

However, the SFG intensity and peak positions are also dependent on surface coverage.[36] Therefore, it is also important to estimate the surface coverage of these monomers at the selected concentration ranges and consider its effect on spectral changes observed with monomers in water. Surface coverage of the monomers at these concentrations are estimated by measuring SFG isotherms.[37−39] A detailed calculation for the surface fractional coverage is shown in the Supporting Information for EMA monomer (Figure S6 and Table S3) for a concentration range of 0−18 mM (spectra not shown). Peak shifts were not observed in the SFG spectra as we increased the concentration from 0 to 18 mM. The minimum to no variation in the SFG intensity profile after ∼7 mM suggests that a full surface coverage was achieved at this

DOI: 10.1021/acs.jpcc.9b07816
J. Phys. Chem. C 2019, 123, 28201−28209

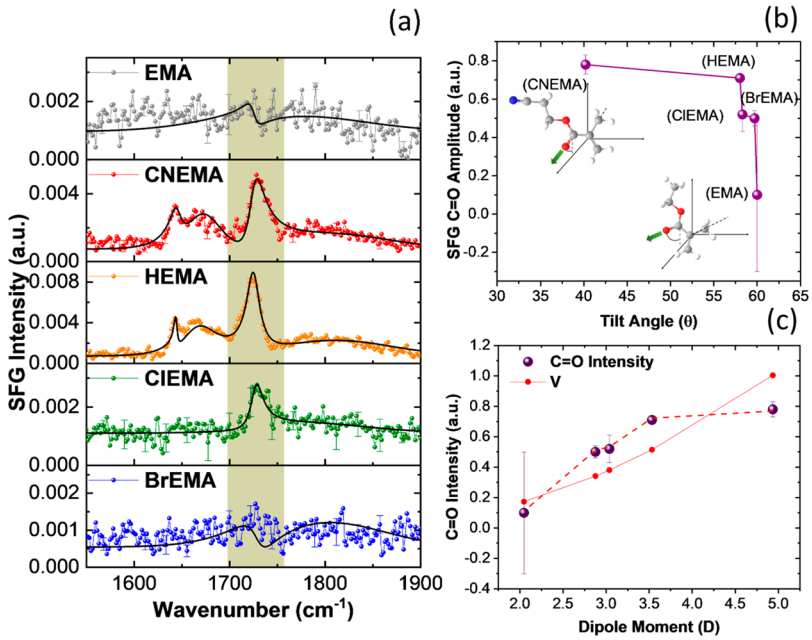

Figure 4. (a) SFG spectra of substituted methacrylate monomers in the C═O vibrational region at the AL interface. Amplitudes of the C═O stretch as a function of (b) tilt angle and (c) dipole moment.

concentration. Similarly, the concentrations at which the full monolayer is formed were estimated by qualitatively evaluating the plots of the SFG intensity of CH_3 vibrational modes as a function of the concentration of CNEMA and BrEMA monomer aqueous solutions. The results for CNEMA monomer imply that a full monolayer has not yet been achieved for the concentration range of 0−12 mM because the SFG intensity of CH_3 FR has not reached a plateau yet, as shown in Figure S7a. The plot of SFG intensity of CH_3 FR for BrEMA monomer as a function of concentration (Figure S7b) shows an inflection point at ∼4 mM which can be considered as the concentration where a full monolayer is obtained.

To summarize, the careful analysis of SFG spectra of EMA monomers in water inferred that the spectral changes from neat monomer to aqueous monomers could be due to interference effects and contribution from $\chi^{(2)}$ or $\chi^{(3)}$ response from water. On the other hand, the CNEMA monomer in water did not show any spectral profile change compared to its neat form, where the CH_3 FR peak was consistently observed at 2935 cm^{-1}. In the case of the BrEMA monomer, it was substantiated that the CH_3 FR peak shift and increased FR interaction were due to the presence of water molecules which then separated the monomer molecules from each other. This further confirmed that the reduction in the FR interaction in neat BrEMA monomer is because of Br and α-CH_3 group being positioned close to each other, which effectively changes the α-CH_3 polarity.

To further examine the surface structure of monomers as a function of substituents, the SSP and PPP SFG spectra were recorded in the C═O vibrational region (1750 cm^{-1}). Figure 4a shows the SSP polarized spectra of monomers at the AL interface. The PPP spectra (Figure S8) and the fitting values and parameters (Table S4) are given in the Supporting Information. In the SSP spectra, the peak at 1725 cm^{-1} is assigned to the C═O stretch.[40] The peak at ∼1640 cm^{-1} observed in the SFG spectra of CNEMA and HEMA monomers is assigned to the C═C stretch of the vinyl group.[28] The SSP spectrum of the EMA monomer (H) did not show any significant signal at the C═O region. However, once the substituents replaced H in EMA, an apparent change in the C═O signal for CNEMA, HEMA, and ClEMA monomers was observed (green highlight, Figure 4a), except for the BrEMA monomer. However, the C═O fitting for the BrEMA monomer reports otherwise, as shown in Table S4. This intensity variation has two possible explanations.

First, we can correlate the change with the estimated tilt angle of the α-CH_3 group because it is closely positioned to the C═O group. SFG signal is reduced when the tilt angle increases from the surface normal based on the IR selection rule. The average tilt angles of the α-CH_3 group of the monomers were calculated using the intensity ratio of α-CH_3 SS (SSP/PPP) (Table S5). The tilt angle values varied with the substituent. However, the estimated deviations (95% confidence level) of the tilt angles are considerably high, which is mainly due to the errors acquired from fitting the spectra. For example, when the α-CH_3 group is oriented close to the surface normal (for CNEMA), the intensity of the C═O vibrational mode is higher, indicating the C═O group is also oriented closer to the surface normal (Figure 4b).

Second, to determine if the intensity variation of the C═O signal at the AL interface is due to either the dipole moment or polarizability; we carried out infrared and Raman bulk measurements. Then, we plotted the fitted C═O signal from both measurements as a function of the fitted SFG C═O signal for all monomers (provided in the Supporting Information, Figure S9a). Based on the results, the IR signal has changed due to the characteristics of the substituents. On the other hand, the Raman did not vary except for the HEMA monomer. This result for HEMA monomers is due to hydrogen bond formation between C═O···HO and OH···OH. Therefore, SFG C═O signal variations in the monomers can be explained by the change in the dipole moment from replacing H with the other substituents. Therefore, to further support these explanations, we used the substituent constants from the review written by Taft and colleagues: specifically, the *F* parameter values of Swain and Lupton built from Hammett's

DOI: 10.1021/acs.jpcc.9b07816
J. Phys. Chem. C 2019, 123, 28201−28209

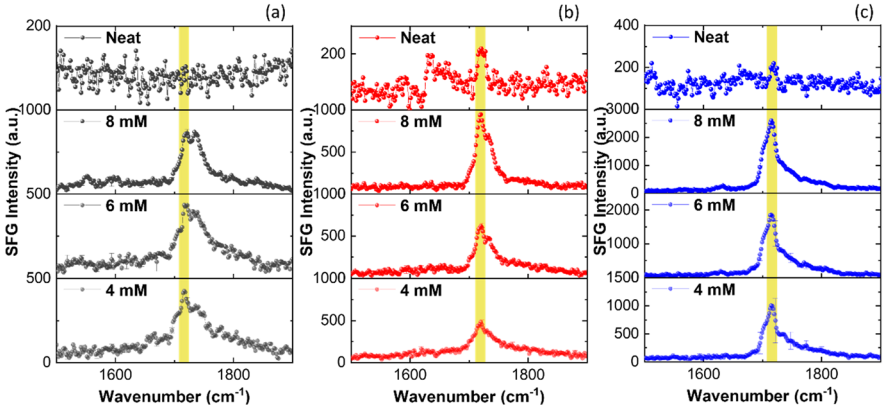

Figure 5. SFG spectra of (a) EMA, (b) CNEMA, and (c) BrEMA in the water at SSP polarization combination in the C═O vibrational region (1750 cm^{-1}). The C═O stretch is indicated with yellow highlight.

parameters.[41] The *F* parameter was derived from the Swain–Lupton equation, which is a linear free energy relationship that can be used to assess the substituent effects.[41] The *F* parameters also only focus on purely inductive effects which are defined by field and electronegativity effects. The plot is shown in Figure S9b, which shows the C═O SFG signal to be dependent on the addition of substituents using the substituent constants. In this case, a slight increase in the C═O signal was acquired when H was substituted by Br, Cl, CN, and OH groups. On the other hand, it evaluates if the surface tension (ST) has a role or an effect on the observation and changes in the SFG intensity of the C═O signal at the AL interface. The surface tension gives an idea about the hydrophobic nature of the neat monomer at the air–liquid interface. At the same time, it can also find the relationship between hydrophobicity and the C═O SFG signal. It seems that, with substituents, there was a slight increase in the surface tension values, which shows the monomers' increasing hydrophilic nature or decreasing hydrophobic nature. Therefore, if the surface tension (~26 mJ/m^2) is lower, as in the case of EMA, more hydrophobic functional groups are arranged closer to the air–liquid interface. In this case, the surface tension picture in relation to the C═O signal only shows an effect upon replacement of H but the C═O signal between Br, Cl, CN, and OH substituted monomers was not greatly affected by the change in their surface tension values. Consequently, surface tension did not show much effect on the SFG signal of α-CH_3 SS and FR peaks. Other than acquiring these estimated tilt angles, *F* parameter comparisons, and ST measurements, we also obtained the overall dipole moment of each monomer using Gaussian 9.0 (B3LYP functional, AUG-cc-PVTZ basis set), as shown in Figure 4c.

Herein, a plot between the SFG C═O signal with respect to the *F* parameter values shows the dependence of the SFG C═O signal on the change of electronic substituents (Figure S9b). In this case, the electronegativity may not play a role in the change in the intensity because the C═O group is separated by an additional two carbon atoms to the substituents which reduce its influence. However, field effects defined by interaction through space is another method that can affect the C═O signal due to the proximity of the substituent. When Br or Cl is near the carbonyl oxygen in space, a higher frequency results relative to the isomer in which the Br or Cl has rotated away from the oxygen.[32] This results in the electron cloud of the Br or Cl atom near the oxygen electrostatically restraining the tendency of the oxygen to attract electrons. Rotational isomers can occur due to the field effect. The C═O group is known to have a strong dipole moment due to the polarity of the double bond; thus, it is highly sensitive toward minor changes in the environment. It can participate in electrostatic interactions through its positively charged carbon and negatively charged oxygen. The ester groups of the monomers are structurally flexible because the C–O–C bond has a low barrier; thus changes in its conformation are possible. In the literature, these conformations are reported to be influenced by the nature of the substituents and solvents if present[42,43] relative to the neighboring polar group.[44] Additionally, since no peak shift to higher frequency was observed, it is less feasible that the intramolecular field induced changes in the C═O signal. However, these explanations still support the changes being due to intermolecular interactions through space where the substituent is still located near the carbonyl group. If this happens, the electron cloud around the substituent electrostatically restrains the tendency of the oxygen atom to receive an electron.

Using the dipole moment values estimated from Gaussian 9.0, the SFG C═O signal shows dependence on the overall dipole moment of monomers at the AL interface. Analogously, we simulated the potential energy of the dipole–dipole interaction to explain the trend in Figure 4c, wherein two polar molecules are positioned near each other. With the following equation

$$V(r, \theta_1, \theta_2, \phi) = -\frac{\mu_1\mu_2}{4\pi\varepsilon_0 r^3}[2\cos\theta_1\cos\theta_2 - \sin\theta_1\sin\theta_2\cos\phi]$$

where V is the potential energy defining this specific interaction, μ_1 and μ_2 are two point dipoles of moments separated at a distance r and oriented relative to each other defined by θ_1 and θ_2, while ϕ is the rotation along the axis perpendicular to the normal. ε_0 is the permittivity of free space: 8.854×10^{-12} C^2 N^{-1} m^{-1}. When the dipoles are aligned in line, a maximum attraction occurs between the two dipoles. However, if these two dipoles are parallel to each other, the dipoles are much closer to each other. Thus, this configuration makes a favorable interaction and leads to the minimization of the potential energy.[45] This selected conformation can represent our observations at the AL interface because of its

DOI: 10.1021/acs.jpcc.9b07816
J. Phys. Chem. C 2019, 123, 28201–28209

connection to preferred SF activity. Therefore, if we assume that the two dipoles are parallel to each other, we can use 90°, 90°, 0° and 0.29 nm for θ_1, θ_2, ϕ, and r values and estimate $V(r,\theta_1,\theta_2,\phi)$.[45] At such parameters, the SFG C═O amplitude and the simulated $V(r,\theta_1,\theta_2,\phi)$ (shown in red line) are both plotted with respect to the dipole moment estimated from the Gaussian 9.0 software. As shown in Figure 4c, the plotted potential energy with respect to the dipole moment is used to describe the dipole−dipole interaction of the neat EMA and substituted monomers at the AL interface. EMA and CNEMA monomers fit the model with a ϕ modification, where ϕ = 50° for EMA and ϕ = 40° for CNEMA monomer. HEMA, ClEMA, and BrEMA monomers fit the model with θ_1 and θ_2 modifications. Values of θ_1 = 150° and θ_2 = 60° are reported for HEMA monomer, whereas θ_1 = 150° and θ_2 = 60° are needed for ClEMA and BrEMA monomers. The results of the readjustments for the parameter values of θ_1, θ_2, and ϕ to fit the acquired SFG C═O data are presented in the red dashed line in Figure 4c.

Earlier, we mentioned our experiment using aqueous solutions of our monomers. We observed hydrogen-bonded water molecules in the OH region (spectra not shown). In addition, the C═O signal was obtained for 4, 6, and 8 mM EMA, CNEMA, and BrEMA monomers in water (Figure 5). The spectral data from neat to aqueous solutions were collected on the same day to avoid discrepancies introduced by collecting data on different days. The preparation of different concentrations of monomers in water was only shown to present the significant change of the C═O signal when present in water in comparison to the C═O signal at the neat state of the monomer. A significant increase is observed when going from neat sample to aqueous samples. As an example, in Figure S10b, the SFG intensity of the C═O vibrational mode was also plotted as a function of concentration of the BrEMA monomers in water (4−8 mM) to show the extent of the change in the C═O signal. In general, Figure S10 shows the intensity variation of C═O stretch for the BrEMA monomer in water at different concentrations; the increasing SFG intensity is due to increasing number density of the C═O vibrational modes at the air−liquid interface. These results indicate only not the ability of the water molecules to form H-bonds but also its ability to create a directional dipole−dipole interaction that augments SF activity.

Therefore, to further investigate the effect of substituents and their interactions in a more controlled condition, we used a hydrophilic fused silica surface to interact with neat monomers. At the solid−liquid interface, we picture the top layer of monomers to be bonded to the available surface silanol groups of the fused silica window, which relatively restricts their arrangement, in comparison to the air−liquid interface, where the liquid has fewer restrictions and is loosely packed.[40] At this interface, hydrogen bonding formation can be mediated between the C═O group of the monomers and the available surface silanol (Si−OH) groups. We hypothesize that the formation of H-bonds should adjust the field effects exerted by the substituents on the molecular groups. The CH vibrational region spectra of the monomers were collected at SSP and PPP polarization combinations. The spectra are given in the Supporting Information (Figure S11) with fitting results and parameters (Tables S6 and S7). The CH region spectra of all the monomers show similar spectral profiles at both SSP and PPP polarization combinations. One key observation at the SL interface is that the FR interaction or signal is not affected by replacing H with CN, OH, Cl, and Br substituents (Figure S12, Supporting Information). Details about the orientation of α-CH_3 group are available in the Supporting Information (Table S8).

Next, the SFG spectra of the monomers were recorded at 1750 cm^{-1} using SSP (Figure 6) and PPP polarization

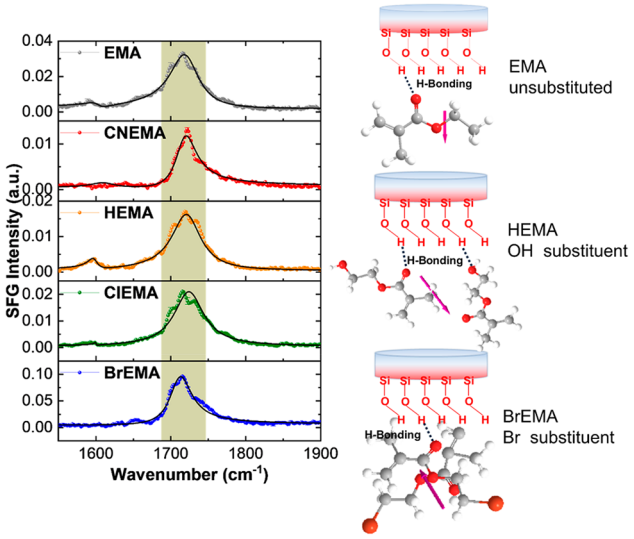

Figure 6. SFG spectra of substituted methacrylate monomers in the C═O vibrational region at the SL interface and a cartoon representation of the monomers at hydrophilic silica−monomer interface emphasizing the formation of hydrogen bonds.

combinations at the SL interface. PPP spectra (Figure S13) and the fitting values and parameters (Table S9) are available in the Supporting Information. In the series of SSP spectra, the C═O stretch is observed at 1720 cm^{-1}.[40] The intensity of the C═O stretch (1720 cm^{-1}) from the fitted spectra varies with the higher value for BrEMA and the lowest value for CNEMA. Plots of the SFG C═O amplitude versus (i) dipole moment values obtained from IR measurement and density functional theory (DFT) (Figure S14a,b, Supporting Information), (ii) surface tension at the SL interface (Figure S14c, Supporting Information), and (iii) F parameter values (substituent constants) of Swain and Lupton (Figure S14d, Supporting Information)[41] were shown to explain the discernible C═O signal at the SL interface. As stated earlier, since we did not obtain the average tilt angle values for the CNEMA and BrEMA monomers; we opted not to plot the C═O signal as a function of the α-CH_3 tilt angle. The replacement of substituents has less effect at the SL interface compared to the results of the AL interface. Looking closely at the plots of SFG C═O signal as a function of the IR C═O signal and the dipole moment from the DFT calculation, the SFG C═O signal from ClEMA and BrEMA monomers varied a little from that of EMA (unsubstituted) monomer. However, CNEMA and HEMA varied a little bit more from EMA when compared to other monomer derivatives. Although the variations are not so apparent, similar results were observed when the C═O signal was plotted against substituent constants and surface tension values. Therefore, the apparent observation of the C═O signal at the SL interface is not only from the microscopic property via dipole moment or using surface tension as a macroscopic measurement. Another interaction that can explain our results is hydrogen bond formation. Since the

DOI: 10.1021/acs.jpcc.9b07816
J. Phys. Chem. C 2019, 123, 28201−28209

carbonyl group is sensitive to changes in the chemical environment, the presence of a silanol group (solid) or surface hydroxyl group, as an oscillator, can selectively interact with the C═O group forming hydrogen bonds (C═O···H−O). In SFG, this localized interaction allows for the C═O group to orient parallel normal to the surface, which results in the enhancement of the signal. However, the intensity is also dependent on the number density of the vibrational modes present at the interface. Thus, this explains why only a slight change was observed in the C═O intensity from the EMA monomer to ClEMA and BrEMA monomers because it is less likely for the −Cl and −Br substituents to form H-bonds with the C═O (intra- and inter-) and the Si−OH group. −Cl and −Br substituents are considered weak to non-H-bonding species. Thus, this situated the C═O group to specifically interact with the OH group and allowed a higher number of C═O groups to interact with the surface hydroxyl groups resulting in higher C═O intensity. However, a different scenario explains the slight reduction in the C═O signal for both HEMA and CNEMA compared to ClEMA and BrEMA. The −CN group of CNEMA can form weak H-bonds with Si−OH group. In addition, the OH group of HEMA can form H-bonds with the available surface silanol group, the C═O, and the OH groups of the HEMA monomer itself. These result in intra- and intermolecular interactions, i.e., C═O···HO−CH_2, H_2C−OH···OH−CH_2, C═O···HO−Si, and Si−OH···OH−CH_2 (Figure 6).

Therefore, based on SFG selection rules, the number of oriented C═O groups to the surface normal, as well as the number density of the C═O stretch, is reduced at the SL interface. Spectroscopically, the broader bandwidth and the intensification of the C═O signal is a result of hydrogen bonding formation (C═O···H−O) between the C═O of the methacrylate-based monomer and the Si−OH group of the hydrophilic fused silica interface.[28]

CONCLUSION

In summary, we have shown that the substituents attached to the ethyl end of a methacrylate backbone, replacing H, affect the overall interfacial monomer conformations at AL and SL interfaces. The SFG spectra of EMA and substituted monomers at the AL interface show variations in the intensity of methyl FR mode relative to the α-CH_3 SS, whereas at the SL interface the intensity of the FR mode is not drastically changed. Moreover, an apparent change in the intensity of the C═O stretch was observed in the presence of substituents, with the highest C═O stretch intensity being observed for CNEMA. On the other hand, the intensity of the C═O stretch varies with a higher fitted value for BrEMA (∼5.4) and the lowest fitted value for CNEMA (∼1.8) at the SL interface. These changes in the conformation were driven by the nature of the substituent, intra- and intermolecular interactions, interfacial properties such as surface tension, and the overall dipole moment of the monomers. In conclusion, this model study of electronic substituents at different interfaces is beneficial to the broad communities of physical organic chemistry, surface science, and materials science in predicting favored interactions in a more complex chemical environment, different interfaces, and developing surface-initiated reactions. The intermolecular and intramolecular interactions of monomers affect macroscopic properties such as viscosity and hence the polymerization kinetics.[46] Therefore, an in-depth understanding of the interfacial methacrylate structure and its interactions can also open a pathway for many other surface research opportunities.

ASSOCIATED CONTENT

Supporting Information

The Supporting Information is available free of charge on the ACS Publications website at DOI: 10.1021/acs.jpcc.9b07816.

Syntheses of monomers, additional SFG spectral data, and fitting parameters (PDF)

AUTHOR INFORMATION

Corresponding Author

*E-mail: cimatu@ohio.edu.

ORCID

Uvinduni I. Premadasa: 0000-0003-0289-2965
Narendra M. Adhikari: 0000-0002-1315-408X
Katherine Leslee A. Cimatu: 0000-0002-4216-9715

Author Contributions

†U.I.P. and N.M.A.: These authors contributed equally.

Notes

The authors declare no competing financial interest.

ACKNOWLEDGMENTS

The authors would like to thank Drs. Hugh Richardson, Eric Masson, Andrew Tangonan, Benjamin Bythell, and Michael Jensen for assistance and in-depth discussions. Also, the authors thank Ahmed Aboelenen for IR characterization, Ali Rafiei for Raman characterization, Gabrielle Chiong and Tharushi Ambagaspitiya for assistance in the artwork. The current work was supported by NSF (Grants CHE-0947031 and CHE-1338000) for the acquisition of the femtosecond laser and nuclear magnetic spectrometer, the start-up fund of the Department of Chemistry and Biochemistry, the College of Arts and Sciences, and the Vice President for Research at Ohio University. Additionally, the authors would like to thank the Nanoscale and Quantum Phenomena Institute for their financial support. U.I.P. was also partially supported by the NSF (Grant CBET-1705817).

REFERENCES

(1) Roberts, J. D.; Moreland, W. T., Jr. Electrical Effects of Substituent Groups in Saturated Systems. Reactivities of 4-Substituted Bicyclo [2.2. 2] Octane-1-Carboxylic Acids1. *J. Am. Chem. Soc.* **1953**, *75*, 2167−2173.

(2) Swain, C. G.; Unger, S. H.; Rosenquist, N. R.; Swain, M. S. Substituent Effects on Chemical Reactivity. Improved Evaluation of Field and Resonance Components. *J. Am. Chem. Soc.* **1983**, *105*, 492−502.

(3) Hollingsworth, C. A.; Seybold, P. G.; Hadad, C. M. Substituent Effects on the Electronic Structure and pKa of Benzoic Acid. *Int. J. Quantum Chem.* **2002**, *90*, 1396−1403.

(4) Costa, G.; Lisciotto, M.; Valenti, B. Structure and Substitution Effects on the Thermotropicity of Some Polyesters and Model Compounds. *Liq. Cryst.* **1992**, *11*, 447−457.

(5) Benjamin, I. Theoretical Study of the Water/1, 2-Dichloroethane Interface: Structure, Dynamics, and Conformational Equilibria at the Liquid−Liquid Interface. *J. Chem. Phys.* **1992**, *97*, 1432−1445.

(6) Streitwieser, A.; Taft, R. W. *Progress in Physical Organic Chemistry*; John Wiley & Sons: 2009; Vol. *10*.

(7) Cyran, J. e. D.; Backus, E. H. G.; Nagata, Y.; Bonn, M. Structure from Dynamics: Vibrational Dynamics of Interfacial Water as a Probe of Aqueous Heterogeneity. *J. Phys. Chem. B* **2018**, *122*, 3667−3679.

DOI: 10.1021/acs.jpcc.9b07816
J. Phys. Chem. C 2019, 123, 28201−28209

(8) Aidarova, S.; Sharipova, A.; Krägel, J.; Miller, R. Polyelectrolyte/Surfactant Mixtures in the Bulk and at Water/Oil Interfaces. *Adv. Colloid Interface Sci.* **2014**, *205*, 87−93.
(9) Gunes, D.; Karagoz, B.; Bicak, N. Synthesis of Methacrylate-Based Functional Monomers Via Boron Ester Acidolysis and Their Polymerization. *Des. Monomers Polym.* **2009**, *12*, 445−454.
(10) Cimatu, K. A.; Chan, S. C.; Jang, J. H.; Hafer, K. Preferential Organization of Methacrylate Monomers and Polymer Thin Films at the Air Interface Using Femtosecond Sum Frequency Generation Spectroscopy. *J. Phys. Chem. C* **2015**, *119*, 25327−25339.
(11) Piradashvili, K.; Alexandrino, E. M.; Wurm, F. R.; Landfester, K. Reactions and Polymerizations at the Liquid−Liquid Interface. *Chem. Rev.* **2016**, *116*, 2141−2169.
(12) Siebert, J. M.; Baier, G.; Musyanovych, A.; Landfester, K. Towards Copper-Free Nanocapsules Obtained by Orthogonal Interfacial "Click" Polymerization in Miniemulsion. *Chem. Commun.* **2012**, *48*, 5470−5472.
(13) Manna, A.; Kumar, A. Why Does Water Accelerate Organic Reactions under Heterogeneous Condition? *J. Phys. Chem. A* **2013**, *117*, 2446−2454.
(14) Aoshima, S.; Kanaoka, S. A Renaissance in Living Cationic Polymerization. *Chem. Rev.* **2009**, *109*, 5245−5287.
(15) Kostjuk, S. V.; Ganachaud, F. Cationic Polymerization of Vinyl Monomers in Aqueous Media: From Monofunctional Oligomers to Long-Lived Polymer Chains. *Acc. Chem. Res.* **2010**, *43*, 357−367.
(16) Shen, Y. R. Basic Theory of Surface Sum-Frequency Generation. *J. Phys. Chem. C* **2012**, *116*, 15505−15509.
(17) Lambert, A. G.; Davies, P. B.; Neivandt, D. J. Implementing the Theory of Sum Frequency Generation Vibrational Spectroscopy: A Tutorial Review. *Appl. Spectrosc. Rev.* **2005**, *40*, 103−145.
(18) Hirose, C.; Akamatsu, N.; Domen, K. Formulas for the Analysis of Sum-Frequency Generation Spectrum by CH Stretching Modes of Methyl and Methylene Groups. *J. Chem. Phys.* **1992**, *96*, 997.
(19) Hirose, C.; Yamamoto, H.; Akamatsu, N.; Domen, K. Orientation Analysis by Simulation of Vibrational SFG Spectrum: CH Stretching Bands of the Methyl Group. *J. Phys. Chem.* **1993**, *97*, 10064.
(20) Wang, H. F.; Gan, W.; Lu, R.; Rao, Y.; Wu, B. H. Quantitiative Spectral and Orientational Analysis in Surface Sum Frequency Generation Vibrational Spectroscopy (SFG-VS). *Int. Rev. Phys. Chem.* **2005**, *24*, 191.
(21) Chan, S. C.; Jang, J. H.; Cimatu, K. A. Orientational Analysis of Interfacial Molecular Groups of a 2-Methoxyethyl Methacrylate Monomer Using Femtosecond Sum Frequency Generation Spectroscopy. *J. Phys. Chem. C* **2016**, *120*, 29358−29373.
(22) Wang, H.-F.; Velarde, L.; Gan, W.; Fu, L. Quantitative Sum-Frequency Generation Vibrational Spectroscopy of Molecular Surfaces and Interfaces: Lineshape, Polarization, and Orientation. *Annu. Rev. Phys. Chem.* **2015**, *66*, 189−216.
(23) Wang, J.; Chen, C.; Buck, S. M.; Chen, Z. Molecular Chemical Structure on Poly (Methyl Methacrylate) (PMMA) Surface Studied by Sum Frequency Generation (SFG) Vibrational Spectroscopy. *J. Phys. Chem. B* **2001**, *105*, 12118−12125.
(24) Premadasa, U. I.; Adhikari, N. M.; Baral, S.; Aboelenen, A. M.; Cimatu, K. L. A. Conformational Changes of Methacrylate-Based Monomers at the Air−Liquid Interface Due to Bulky Substituents. *J. Phys. Chem. C* **2017**, *121*, 16888−16902.
(25) Hirata, T.; Matsuno, H.; Kawaguchi, D.; Yamada, N. L.; Tanaka, M.; Tanaka, K. Effect of Interfacial Structure on Bioinert Properties of Poly (2-Methoxyethyl Acrylate)/Poly (Methyl Methacrylate) Blend Films in Water. *Phys. Chem. Chem. Phys.* **2015**, *17*, 17399−17405.
(26) Jakobsen, R. J.; Mikawa, Y.; Allkins, J. R.; Carlson, G. L. The Vibrational Spectra of Propanoic Acid. *J. Mol. Struct.* **1971**, *10*, 300−303.
(27) Yu, Y.; Lin, K.; Zhou, X.; Wang, H.; Liu, S.; Ma, X. New C− H Stretching Vibrational Spectral Features in the Raman Spectra of Gaseous and Liquid Ethanol. *J. Phys. Chem. C* **2007**, *111*, 8971−8978.
(28) Larkin, P. *Infrared and Raman Spectroscopy: Principles and Spectral Interpretation*; Elsevier: 2011.
(29) Ishiyama, T.; Sokolov, V. V.; Morita, A. Molecular Dynamics Simulation of Liquid Methanol. II. Unified Assignment of Infrared, Raman, and Sum Frequency Generation Vibrational Spectra in Methyl C−H Stretching Region. *J. Chem. Phys.* **2011**, *134*, 024510.
(30) Tian, K.; Zhang, B.; Ye, S.; Luo, Y. Intermolecular Interactions at the Interface Quantified by Surface-Sensitive Second-Order Fermi Resonant Signals. *J. Phys. Chem. C* **2015**, *119*, 16587−16595.
(31) Malyk, S.; Shalhout, F. Y.; O'Leary, L. E.; Lewis, N. S.; Benderskii, A. V. Vibrational Sum Frequency Spectroscopic Investigation of the Azimuthal Anisotropy and Rotational Dynamics of Methyl-Terminated Silicon (111) Surfaces. *J. Phys. Chem. C* **2013**, *117*, 935−944.
(32) Colthup, N. *Introduction to Infrared and Raman Spectroscopy*; Elsevier: 2012.
(33) Ward, R. N. *Sum-Frequency Spectroscopy of Molecules at Interfaces*. Ph.D. Thesis, University of Cambridge, 1993.
(34) Dogangun, M.; Ohno, P. E.; Liang, D.; McGeachy, A. C.; Be, A. G.; Dalchand, N.; Li, T.; Cui, Q.; Geiger, F. M. Hydrogen-Bond Networks near Supported Lipid Bilayers from Vibrational Sum Frequency Generation Experiments and Atomistic Simulations. *J. Phys. Chem. B* **2018**, *122*, 4870.
(35) Adams, A. J. *Sum Frequency Generation Spectroscopy of Simulated Protein Secondary Structures*. Master's Thesis, University of Louisville, Louisville, KY, 2018.
(36) Westerberg, S.; Wang, C.; Somorjai, G. A. Heat of Adsorption of Co on Pt (1 1 1) Obtained by Sum Frequency Generation Vibrational Spectroscopy -a New Technique to Measure Adsorption Isotherms. *Surf. Sci.* **2005**, *582*, 137−144.
(37) Wang, C.-y.; Groenzin, H.; Shultz, M. J. Comparative Study of Acetic Acid, Methanol, and Water Adsorbed on Anatase Tio2 Probed by Sum Frequency Generation Spectroscopy. *J. Am. Chem. Soc.* **2005**, *127*, 9736−9744.
(38) Weißenborn, E.; Braunschweig, B. Specific Ion Effects of Dodecyl Sulfate Surfactants with Alkali Ions at the Air−Water Interface. *Molecules* **2019**, *24*, 2911.
(39) Johnson, C. M.; Tyrode, E. Study of the Adsorption of Sodium Dodecyl Sulfate (SDS) at the Air/Water Interface: Targeting the Sulfate Headgroup Using Vibrational Sum Frequency Spectroscopy. *Phys. Chem. Chem. Phys.* **2005**, *7*, 2635−2640.
(40) Adhikari, N. M.; Premadasa, U. I.; Cimatu, K. L. A. Sum Frequency Generation Vibrational Spectroscopy of Methacrylate-Based Functional Monomers at the Hydrophilic Solid-Liquid Interface. *Phys. Chem. Chem. Phys.* **2017**, *19*, 21818−21828.
(41) Hansch, C.; Leo, A.; Taft, R. W. A Survey of Hammett Substituent Constants and Resonance and Field Parameters. *Chem. Rev.* **1991**, *91*, 165−195.
(42) Pawar, D. M.; Khalil, A. A.; Hooks, D. R.; Collins, K.; Elliott, T.; Stafford, J.; Smith, L.; Noe, E. A. E and Z Conformations of Esters, Thiol Esters, and Amides. *J. Am. Chem. Soc.* **1998**, *120*, 2108−2112.
(43) Dugave, C.; Demange, L. Cis-Trans Isomerization of Organic Molecules and Biomolecules: Implications and Applications. *Chem. Rev.* **2003**, *103*, 2475−2532.
(44) Sahariah, B.; Sarma, B. K. Relative Orientation of the Carbonyl Groups Determines the Nature of Orbital Interactions in Carbonyl−Carbonyl Short Contacts. *Chem. Sci.* **2019**, *10*, 909.
(45) Israelachvili, J. N. *Intermolecular and Surface Forces*; Academic Press: 2011.
(46) Lemon, M. T.; Jones, M. S.; Stansbury, J. W. Hydrogen Bonding Interactions in Methacrylate Monomers and Polymers. *J. Biomed. Mater. Res., Part A* **2007**, *83A*, 734−746.

DOI: 10.1021/acs.jpcc.9b07816
J. Phys. Chem. C 2019, 123, 28201−28209